

CONTRACTOR REPORT

SAND98-1750
Unlimited Release



Elastic Tailoring of a Composite D-Spar

Progress Report for Calendar Year 1998

RECEIVED
OCT 01 1998
OSTI

Cheng-Huat Ong and Stephen W. Tsai

Department of Aeronautics and Astronautics
Stanford University
Stanford, CA 94305-4035

Prepared by Sandia National Laboratories Albuquerque, New Mexico 87185
and Livermore, California 94550 for the United States Department of Energy
under Contract DE-AC04-94AL85000

Printed August 1998

Issued by Sandia National Laboratories, operated for the United States Department of Energy by Sandia Corporation.

NOTICE: This report was prepared as an account of work sponsored by an agency of the United States Government. Neither the United States Government nor any agency thereof, nor any of their employees, nor any of their contractors, subcontractors, or their employees, makes any warranty, express or implied, or assumes any legal liability or responsibility for the accuracy, completeness, or usefulness of any information, apparatus, product, or process disclosed, or represents that its use would not infringe privately owned rights. Reference herein to any specific commercial product, process, or service by trade name, trademark, manufacturer, or otherwise, does not necessarily constitute or imply its endorsement, recommendation, or favoring by the United States Government, any agency thereof or any of their contractors or subcontractors. The views and opinions expressed herein do not necessarily state or reflect those of the United States Government, any agency thereof or any of their contractors.

Printed in the United States of America. This report has been reproduced directly from the best available copy.

Available to DOE and DOE contractors from
Office of Scientific and Technical Information
PO Box 62
Oak Ridge, TN 37831

Prices available from (615) 576-8401, FTS 626-8401

Available to the public from
National Technical Information Service
US Department of Commerce
5285 Port Royal Rd
Springfield, VA 22161

NTIS price codes
Printed copy: A03
Microfiche copy: A01

DISCLAIMER

**Portions of this document may be illegible
electronic image products. Images are
produced from the best available original
document.**

SAND98-1750
Unlimited Release
Printed August 1998

Elastic Tailoring of a Composite D-Spar Progress Report for Calendar Year 1998

Cheng-Huat Ong and Stephen W. Tsai
Department of Aeronautics and Astronautics
Stanford University
Stanford, CA 94305-4035

Sandia Contract: BB-6066

ABSTRACT

There are many potential benefits to be gained from the aeroelastic behavior of a wind-turbine blade with bend-twist coupling. However, the ability to manufacture blades with sufficient coupling to provide the desired benefits has yet to be established. This report investigates the feasible (or practical) range of the coupling coefficient that can be obtained on a uniform cross-section composite D-spar, which could be the backbone of a wind-turbine-blade. The most critical parameters are identified and studied across a range of possible values. Various features, such as the geometry, skin thickness, ply distribution, ply materials, and ply orientations, are evaluated for their effect on twist-bend coupling of a D-spar. It is found that sufficient coupling can be built in to the D-spar shape, but that carbon-fiber composite plies angled between 15 and 30 degrees to the longitudinal axis may be required.

.....

Elastic Tailoring of a Composite D-Spar

INTRODUCTION

This report is one of the deliverables of the "Elastic Tailoring of a Composite D-Spar" project. For this deliverable we had to assess the range of the α interaction parameter (bend-twist coupling) for a D-spar structure. It was also essential to identify the critical parameters that affect the range of α .

BRIEF LITERATURE REVIEW

In searching the literature we found that researchers are exploring the potential benefits of the anisotropy of composite materials. A composite design that exhibits various degrees of anisotropy appears to have potential use in rotor blades to reduce vibration, enhance aeroelastic stability and improve aerodynamic efficiency. One of the applications of aeroelastic tailoring is the use of a bend-twist coupled composite wing to prevent divergence of the forward swept wing [1]. Weisshaar [1] also highlighted other potential benefits, such as load relief, vibration control and increase of lift coefficients, resulting from the application of bend-twist coupling.

Smith [2] formulated an analytical model for composite box-beams in the shape of a rectangle or square for rotor blade application. His model can predict the behavior of the composite box-beams that exhibit bend-twist or extension-twist coupling. His analytical results agreed generally well with the results of the Finite Element Model (FEM) and the experimental model [3]. The highlight of the findings is that torsion-related out-of-plane warping can substantially influence torsion and coupled torsion deformations in a symmetric lay-up box-beam.

The application of elastic (or aeroelastic) tailoring for composite structures is not limited to the fixed wing and rotor blade. Kooijman [4] applied it to the wind-turbine-blade for wind energy applications. He investigated the optimum bending-torsion flexibility of the rotor blade for the specific power performance of a rotor. Lobitz [5] also studied one aspect of aeroelastic behavior of bend-twist coupling for wind-turbine-blades. His work indicates

that the aeroelastic behavior of the blade is governed by an interaction parameter, $\alpha = \frac{g}{\sqrt{EI * GK}}$, where g is the coupling stiffness.

Our work is a follow-up to Lobitz's work. We want to know the range of the interaction parameter, α , that can be realized from an actual tailored laminate structure, such as a D-spar.

THEORETICAL ESTIMATION

Instead of immediately performing a numerical estimation of the α interaction parameter for the D-spar, we explored the possibility of estimating the maximum value of the α interaction parameter theoretically to gain some physical insight into bend-twist and extension-twist coupling.

We assume the problem we are looking at is a two-dimensional flat laminate and the in-plane normal stress in the '2' direction has the value of zero, i.e., $\sigma_2 = 0$ (the notation is defined by Tsai [6]).

The constituent relationship between stress and strain is

$$\begin{bmatrix} \sigma_1 \\ \sigma_2 \\ \sigma_6 \end{bmatrix} = \begin{bmatrix} Q_{11} & Q_{12} & Q_{16} \\ Q_{21} & Q_{22} & Q_{26} \\ Q_{61} & Q_{62} & Q_{66} \end{bmatrix} \begin{bmatrix} \varepsilon_1 \\ \varepsilon_2 \\ \varepsilon_6 \end{bmatrix} \quad (1)$$

If $\sigma_2 = 0$, we can reduce the Q matrix as follows,

$$\begin{bmatrix} \sigma_1 \\ \sigma_6 \end{bmatrix} = \begin{bmatrix} \bar{Q}_{11} & \bar{Q}_{16} \\ \bar{Q}_{61} & \bar{Q}_{66} \end{bmatrix} \begin{bmatrix} \varepsilon_1 \\ \varepsilon_6 \end{bmatrix}$$

where

$$\bar{Q}_{11} = Q_{11} - \frac{Q_{12} * Q_{21}}{Q_{22}}$$

$$\bar{Q}_{16} = Q_{16} - \frac{Q_{12} * Q_{26}}{Q_{22}}$$

$$\bar{Q}_{61} = Q_{61} - \frac{Q_{62} * Q_{21}}{Q_{22}}$$

$$\bar{Q}_{66} = Q_{66} - \frac{Q_{62} * Q_{26}}{Q_{22}} \quad (2)$$

The relationship between the in-plane strains $(\varepsilon_1^0, \varepsilon_6^0)$, (κ_1, κ_6) and N_1, N_6, M_1, M_6 is as follows

$$\begin{bmatrix} N_1 \\ N_6 \\ M_1 \\ M_6 \end{bmatrix} = \begin{bmatrix} \bar{A}_{11} & \bar{A}_{16} & \bar{B}_{11} & \bar{B}_{16} \\ \bar{A}_{61} & \bar{A}_{66} & \bar{B}_{61} & \bar{B}_{66} \\ \bar{B}_{11} & \bar{B}_{61} & \bar{D}_{11} & \bar{D}_{16} \\ \bar{B}_{16} & \bar{B}_{66} & \bar{D}_{61} & \bar{D}_{66} \end{bmatrix} \begin{bmatrix} \varepsilon_1^0 \\ \varepsilon_6^0 \\ \kappa_1 \\ \kappa_6 \end{bmatrix} \quad (3)$$

where

$$\bar{A}_{ij} = \int \bar{Q}_{ij} dz$$

$$\bar{B}_{ij} = \int \bar{Q}_{ij} * z dz$$

$$\bar{D}_{ij} = \int \bar{Q}_{ij} * z^2 dz$$

$\varepsilon_1^0, \varepsilon_6^0$: in-plane normal and shear strains

κ_1, κ_6 : bending and twisting curvatures

N_1, N_6 : in-plane normal force and shear force per unit width

M_1, M_6 : bending moment and twisting moment per unit width

Z : the vertical distance between the mid-plane and the ply layer

For a symmetric (symmetry with respect to the mid-plane) laminate, the relation reduces to

$$\begin{bmatrix} N_1 \\ N_6 \\ M_1 \\ M_6 \end{bmatrix} = \begin{bmatrix} \bar{A}_{11} & \bar{A}_{16} & 0 & 0 \\ \bar{A}_{61} & \bar{A}_{66} & 0 & 0 \\ 0 & 0 & \bar{D}_{11} & \bar{D}_{16} \\ 0 & 0 & \bar{D}_{61} & \bar{D}_{66} \end{bmatrix} \begin{bmatrix} \varepsilon_1^0 \\ \varepsilon_6^0 \\ \kappa_1 \\ \kappa_6 \end{bmatrix} \quad (4)$$

For the symmetric laminate, there are two types of coupling:

- a. Extension – Shear coupling

b. Bend – Twist coupling.

For the anti-symmetric laminate, the relation reduces to

$$\begin{bmatrix} N_1 \\ N_6 \\ M_1 \\ M_6 \end{bmatrix} = \begin{bmatrix} \bar{A}_{11} & 0 & 0 & \bar{B}_{16} \\ 0 & \bar{A}_{66} & \bar{B}_{61} & 0 \\ 0 & \bar{B}_{61} & \bar{D}_{11} & 0 \\ \bar{B}_{16} & 0 & 0 & \bar{D}_{66} \end{bmatrix} \begin{bmatrix} \varepsilon_1^0 \\ \varepsilon_6^0 \\ \kappa_1 \\ \kappa_6 \end{bmatrix} \quad (5)$$

In this case, the coupling is different from the previous case. The couplings are,

a. Extension – Twist coupling

b. Bend – Shear coupling.

If the laminates are not symmetric or anti-symmetric, there will be more than two modes of coupling. The stiffness and compliance matrix will be fully populated.

How do the \bar{A}_{ij} , \bar{B}_{ij} , \bar{D}_{ij} values relate to the “EI”, “GJ” and “g” of Lobitz’s work? Let us reprint some of the equations in Lobitz’s work [5] that are applicable to our derivation.

The equations that Lobitz used for the extension-twist coupling are given in matrix form below:

$$\begin{bmatrix} EA & -g \\ -g & GK \end{bmatrix} \begin{bmatrix} \frac{\partial u}{\partial x} \\ \frac{\partial \varphi}{\partial x} \end{bmatrix} = \begin{bmatrix} F \\ M_t \end{bmatrix} \quad (\text{Equation 1 in Reference [5]})$$

$$\begin{bmatrix} EI & -g \\ -g & GK \end{bmatrix} \begin{bmatrix} \frac{\partial \theta}{\partial x} \\ \frac{\partial \varphi}{\partial x} \end{bmatrix} = \begin{bmatrix} M_b \\ M_t \end{bmatrix} \quad (\text{Equation 6 in Reference [5]})$$

The terms are defined in Lobitz’s paper [5]. The $\frac{\partial u}{\partial x}$ is our ε_1^0 ; the $\frac{\partial \theta}{\partial x}$ is our κ_1 ; the $\frac{\partial \varphi}{\partial x}$ is our κ_6 . For the forces, the F is our $b \cdot N_1$; the M_t is our $b \cdot M_6$ and the M_b is our $b \cdot M_1$. The parameter “b” is the width of the flat laminate.

The “EI”, “GK”, “g” can be expressed by A_{ij} , B_{ij} and D_{ij} as follows:

Bend-Twist Coupling (Symmetry)

$$\bar{D}_{11} = \frac{EI}{b}$$

$$\bar{D}_{66} = \frac{GK}{b}$$

$$\bar{D}_{16} = -\frac{g}{b}$$

$$\alpha = \frac{g}{\sqrt{EI * GK}} = -\frac{\bar{D}_{16}}{\sqrt{\bar{D}_{11} * \bar{D}_{66}}}$$

where b is the width of the laminate.

If the laminate has a lay-up of $[\theta]_s$ (single orientation), the α is further reduced to

$$\alpha = -\frac{\bar{Q}_{16}}{\sqrt{\bar{Q}_{11} * \bar{Q}_{66}}} = -\frac{Q_{16} * Q_{22} - Q_{12} * Q_{26}}{\sqrt{(Q_{11} * Q_{22} - Q_{12}^2) * (Q_{66} * Q_{22} - Q_{26}^2)}} \quad (6)$$

Extension-Twist Coupling (Antisymmetry)

$$\bar{A}_{11} = \frac{EA}{b}$$

$$\bar{D}_{66} = \frac{GK}{b}$$

$$\bar{B}_{16} = -\frac{g}{b}$$

$$\alpha = \frac{g}{\sqrt{EI * GK}} = -\frac{\bar{B}_{16}}{\sqrt{\bar{A}_{11} * \bar{D}_{66}}}$$

If the laminate has a lay-up of $[\theta]_{AS}$ (single orientation), the α is further reduced to

$$\begin{aligned}\alpha &= -\sqrt{\frac{3}{4}} * \frac{\bar{Q}_{16}}{\sqrt{\bar{Q}_{11} * \bar{Q}_{66}}} \\ &= -\sqrt{\frac{3}{4}} * \frac{Q_{16} * Q_{22} - Q_{12} * Q_{26}}{\sqrt{(Q_{11} * Q_{22} - Q_{12}^2) * (Q_{66} * Q_{22} - Q_{26}^2)}}\end{aligned}\quad (7)$$

The α interaction parameters for the balanced laminate are related to the normal coupling coefficient (v_{16}) and the shear coupling coefficient (v_{61}). From Reference [6], the two coefficients are defined as follows:

$$\begin{aligned}v_{16} &= \frac{Q_{12} * Q_{26} - Q_{22} * Q_{16}}{Q_{11} * Q_{22} - Q_{12}^2} \\ v_{61} &= \frac{Q_{12} * Q_{26} - Q_{22} * Q_{16}}{Q_{22} * Q_{66} - Q_{26}^2}\end{aligned}\quad (8)$$

Therefore, the α interaction parameters are reduced to the simplest form:

Bend-Twist Coupling

$$\alpha^2 = v_{16} * v_{61}\quad (9)$$

Extension-Twist Coupling

$$\alpha^2 = \frac{3}{4} * v_{16} * v_{61}\quad (10)$$

It is interesting to note that after all the algebraic manipulations, we have obtained a simple form for the α interaction parameter for a flat-plate laminate. This leads to some physical insights: first, the interaction parameter, α , is highly dependent on the ply material, since both the v_{16} and v_{61} coefficients are material-dependent; second, the geometry parameters do not appear in the simplified equation. This implies that the geometrical parameters may not affect the determination of the range of the α . However, for the second observation, we are dealing with a simple type of laminate; that is a flat surface, symmetric or anti-symmetric laminate.

Now let us look at two typical ply materials: a) T800/3900-2 (Graphite/Epoxy) and b) Scotchply (Glass/Epoxy). The ply properties are given in Table 1 below.

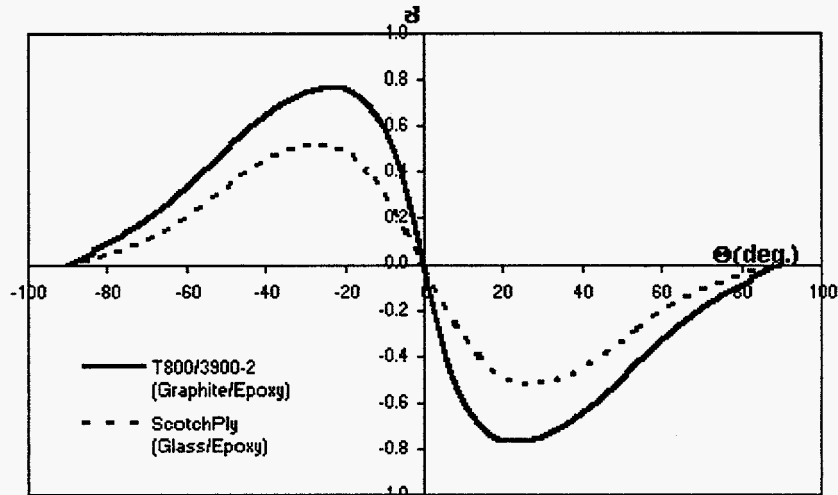
Description	T800/3900-2 (Graphite/Epoxy)	Scotchply (Glass/Epoxy)
E_x (msi)	23.2	5.6
E_y (msi)	1.0	1.2
E_s (msi)	0.9	0.66
ν_x	0.28	0.3

Table 1 The Ply Properties of T800/3900-2 and Scotchply

E_x is the elastic modulus of the ply in the x (longitudinal axis of the fiber) direction. E_y is the elastic modulus of the ply in the y (transverse) direction. And E_s refers to the shear modulus of the ply. The relationship between the ply properties and the laminate properties are defined in reference [6].

The α interaction parameters for these two types of materials are shown in Figure 1 below.

Figure 1 The α Interaction Parameter for T800H/3900-2 and Scotchply Material



It is clearly seen that the range of α interaction parameters depends very much on the type of material chosen. Graphite/Epoxy has a maximum value close to 0.8; and Glass/Epoxy has a maximum value close to 0.5. The maximum values of α for these materials occur at different ply orientations. In general, we can state that the higher values of α occur in ply orientation, θ , between 15° and 30° .

In subsequent sections, we will look into other parameters that affect the α interaction parameters numerically.

NUMERICAL ESTIMATION

Geometry of D-spar

In the numerical study, we study a D-spar composite structure, which is part of the airfoil shape. The basic dimension of the D-spar is 6" (long), 6" (wide) and 3" (height) as shown in Figure 2 below.

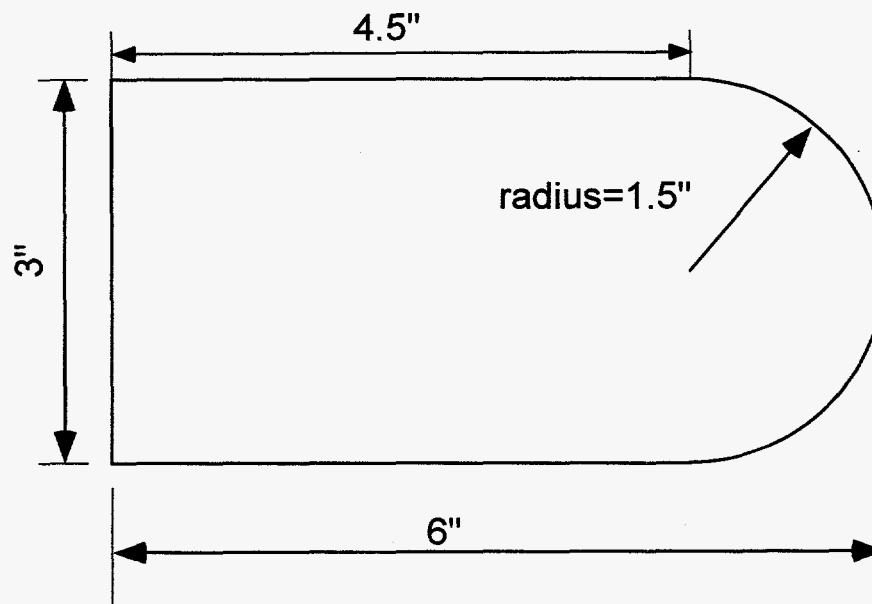


Figure 2 D-spar Cross-Section Shape

The radius of the semi-circle is 1.5". Effectively, the width of the horizontal surface is 4.5".

The lay-up sequence of the top and bottom surface affects the lay-up sequence of the left vertical and right semi-circular walls. If the top and bottom are symmetric lay-ups, then the lay-up of the two walls will be anti-symmetric. On the other hand, if the top and bottom are anti-symmetric lay-ups, then the lay-up of the two walls will be symmetric.

We also need to standardize the lay-up notation. The notation $[\theta_n]_s$ refers to 'n' layers of θ ply, and the subscript 's' denotes that the lay-up is symmetric in reference to the mid-plane between top and bottom surfaces. The notation

$[\theta_n]_{AS}$ refers to 'n' layers of θ ply, and the subscript 'AS' denotes that the lay-up is anti-symmetric in reference to the mid-plane between top and bottom surfaces.

Parametric Study

In this parametric study we investigate various parameters that affect the range of α interaction parameters (mainly for Bend-Twist coupling). The parameters that we have considered are:

- a. geometry
- b. ply materials (Graphite/Epoxy and Glass/Epoxy)
- c. laminate thickness
- d. volumetric fraction of the anisotropy
- e. internal spar or rib
- f. hybrid materials
- g. mixtures of extension-twist and bend-twist lay up
- h. torsion related warping
- i. others such as
 - i) configurations that exhibit the same " α " but which have different "EI" and "GJ"
 - ii) configurations that exhibit different " α " but have the same "EI" and "GJ"

Geometry Effect

We looked into two different cross-sectional dimensions of the D-spar: a) 6" x 3" and b) 6" x 4". The results are shown in Figure 3a. The α interaction parameter does change as we change the height of the D-spar. However, the variation is negligible.

A relevant case for wind turbine blades is to compare the D-spar to an airfoil shape. We compute the α interaction parameter for a 3-inch thick NACA0012 airfoil (25" chord) and compare the results against the 6" x 3" D-spar. We observe that there are negligible effects from the geometry factor in the case of the thin-wall assumption as seen in Figure 3b.

We assume that the transverse shear across the thickness is negligible in the thin-wall case. On the other hand, the transverse shear effect is included in the thick-wall formulation. This leads to increasing the torsion rigidity of the D-

spar and results in a smaller α as seen in Figure 3b. Since the wall thickness (0.2" to 0.3") of the D-spar is small as compared to the height (3" to 4") of the D-spar, the thin-wall formulation is more appropriate .

Material Effect

From the theoretical estimation of the α interaction parameter, we find that the α is highly dependent on the types of material used. For the D-spar, we also expect to see significant effect of the material as we look at both the Graphite/Epoxy and Glass/Epoxy. The numerical results are shown in Figure 4. The maximum α achievable for the graphite and glass materials is 0.62 and 0.42 respectively. The results indicate that the ratio of the maximum α for the two materials is about 3/2 (Graphite/Glass).

Thickness Effect

We have two approaches to studying the effects of the laminate thickness. The first approach is to fix the ply distribution, but to increase or decrease the total laminate thickness. For example, if we have a $[\theta_n/\phi_m]_s$ laminate, the distribution ratio is n/m (or m/n). If we assume each ply has the same thickness (t), then the total thickness is $(m+n)*t$. We proceed with changing the total thickness by varying the "m", "n" layers of plies but keeping the distribution ratio (n/m or m/n) constant. With this arrangement, we see that the α interaction parameter remains constant as shown in Figure 5 (upper half).

The second approach is to keep the total laminate thickness constant and vary the distribution ratio. We looked into various configurations. We observed that the α interaction parameter varies with the distribution ratio as in Figure 5 (lower half).

Anisotropy Volumetric Effect

Figure 5 indicates that the volumetric distribution of the ply within the laminate has a dominant effect on the α interaction parameter. To further study this effect we looked into a laminate that has ply orientation, $[20_n/[45/-45]_m]_s$, where $m=2, 3, 4$. We then varied the parameter 'n' to simulate change in the total thickness as well as the distribution ratio (we defined a $V_a = n/(2*m+n)$). The results are shown in Figure 6. The upper portion of the figure shows that for the same number of 20° plies but different values of V_a , we have different values of α . However, if we adjust the number of layers of 20° plies (n) in such a way that the three configurations have the same value of V_a , we will get a single value of α as seen in the lower portion of Figure 6.

Therefore, for a laminate with a fixed set of ply orientations, the α interaction parameter for that laminate is determined by the volume fraction of the anisotropic plies regardless of distribution ratio.

Internal Spar Effects

An internal spar is inserted at the end-edge of the semi-circle as shown in Figure 7 below.

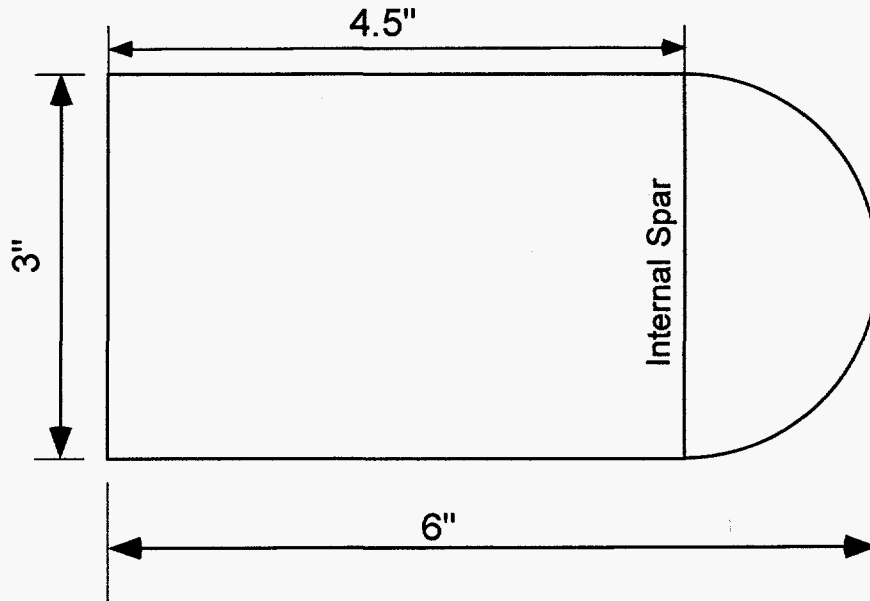


Figure 7 The Cross-Section Dimension of the D-spar with Internal Spar

The insertion of an internal spar will increase the “EI” and “GJ”, and will result in a reduction of the α interaction parameter. We look into both the effects of the thickness and ply orientation of the internal spar. If we increase the thickness of the internal spar while having the same ply orientation, the α interaction parameter reduces, as shown in Figure 8.

The next case considered the constant thickness of the internal spar while varying the ply orientation of the internal spar. The result is shown in Figure 9a. The result indicates that the ply orientation of the D-spar has small effects on the α interaction parameter. The variation of the α interaction parameter with and without an internal spar is about 10%.

In fact, the largest effect of the internal spar is on the lead-lag mode of the D-spar. The D_{ij} of the D-spar with and without an internal spar (same thickness but different orientation) is shown in Figure 9b. We can see that the D_{22} (lead-lag) changes substantially.

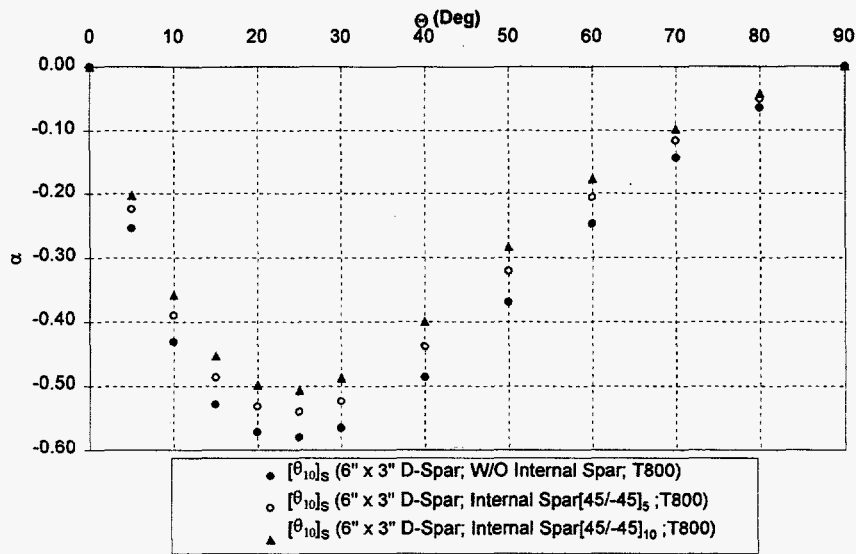


Figure 8 The Effect of Internal Spar Thickness (D-spar Lay-up: $[\theta_{10}]_s$)

Hybrid Materials Effect

To study this effect, we looked at three baseline configurations and compared their results against the same configurations with hybrid material (for all the cases we substituted graphite/epoxy for glass/epoxy). The three configurations we studied are $[\theta(T800)_5/\theta(\text{Scotchply})_5]_s$, $[\theta(T800)_5/0(\text{Scotchply})_5]_s$, $[\theta(T800)_5/90(\text{Scotchply})_5]_s$ and the results are shown in Figure 10.

In the first case, we have 50% graphite fibers and 50% glass fibers all at the same ply orientation. The α interaction parameter of this hybrid case should be lower than the all graphite case and higher than the all glass case (shown in Figure 10). Therefore, the reduction or increase of α depends on the baseline configurations. The lower bound of the α interaction parameter is limited by the low-performance fibers (glass) and the upper bound is limited by the high-performance fibers (graphite).

In the second case, the change is at the 0° material. We replaced 0° graphite fibers with 0° glass fibers or vice versa. The substantial change in α comes mainly from a large change in "EI" as the ratio of the E_x (graphite/fiber) is about 4 to 1. We can deduce that if the volume fraction of non-anisotropic fibers is of lower stiffness than the anisotropic ones, then we can achieve a higher α value.

In the third case, the change is at the 90° material. We replaced 90° graphite fibers with 90° glass fibers or vice versa. The change in α is marginal as there is marginal change in the E_y (transverse ply stiffness) and the E_s (shear modulus) for both materials.

In fact, the dominant effect of using hybrid materials is the significant change in flapping stiffness as shown in Figure 11. Note that the change of D_{12} cannot be seen in the figure as the change is small.

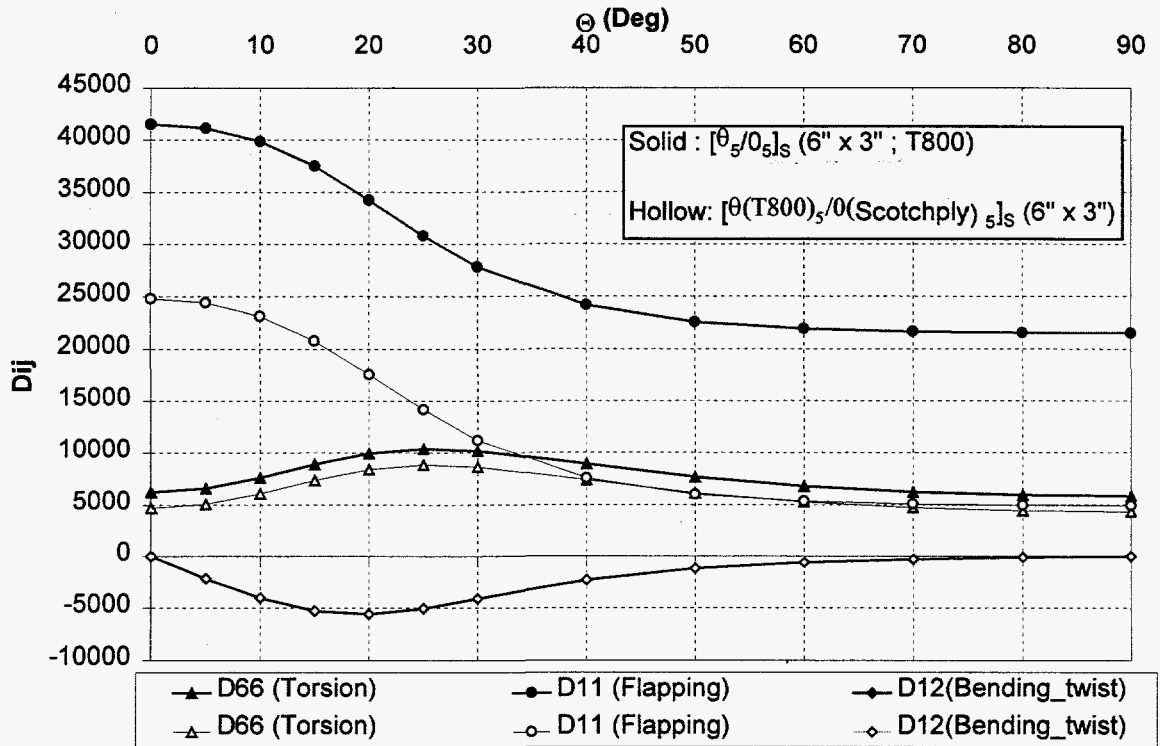


Figure 11 The Effect of Hybrid Materials on D_{ij}

The Effect of Mixtures of Antisymmetric and Symmetric Lay-Ups

Until now we have been looking at a D-spar with symmetric lay-up, and the behavior of the D-spar is quite clear (bend-twist or tension-shear mode). If we replace some of the symmetric lay-up with an anti-symmetric lay-up, the behavior of the D-spar will be very complicated. The following matrices show the change in stiffness matrix from the symmetric ply lay-up to the mixture of symmetric and antisymmetric ply lay-up.

$$\begin{bmatrix} \bar{A}_{11} & \bar{A}_{16} & 0 & 0 \\ \bar{A}_{61} & \bar{A}_{66} & 0 & 0 \\ 0 & 0 & \bar{D}_{11} & \bar{D}_{16} \\ 0 & 0 & \bar{D}_{61} & \bar{D}_{66} \end{bmatrix} \rightarrow \begin{bmatrix} A_{11} & A_{16} & 0 & B_{16} \\ A_{61} & A_{66} & B_{61} & 0 \\ 0 & B_{61} & D_{11} & D_{16} \\ B_{16} & 0 & D_{61} & D_{66} \end{bmatrix}$$

Symmetry

→

mixture [symmetry & antisymmetry]

Instead of bend-twist coupling for the symmetric lay-up, we have complex coupling among bend, twist and shear modes. In fact, the compliance matrix of this mixture is fully populated, therefore it is difficult to control the desired mode of coupling. In addition to that, the α interaction parameter reduces as we increase the degree of mixture as shown in Figure 12. The insertion of core is just for the clarification of the notation, and it does not affect the calculation. The term "core" signifies that the D-spar is hollow.

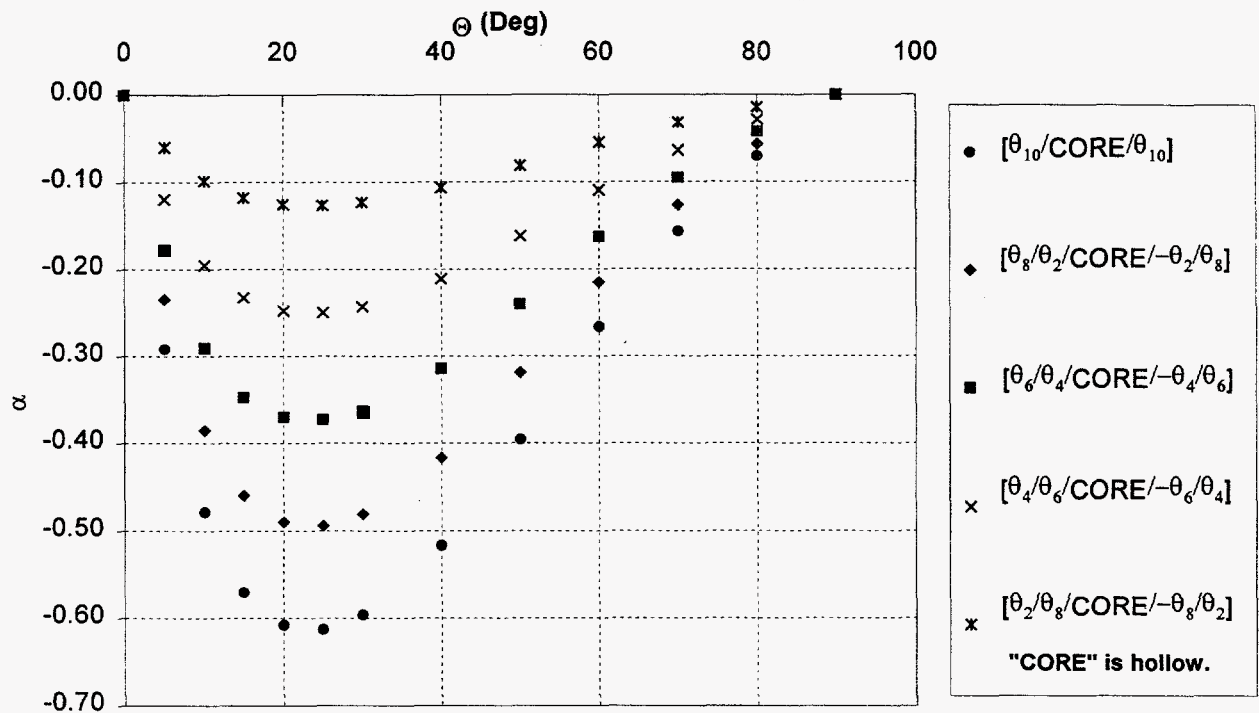


Figure 12 The Effects of Antisymmetry on α Interaction Parameter

Torsion Related Warping

The effect of warping on the α interaction parameter is hard to evaluate. The reason is that it is difficult to include a warping function applicable to all cases in the 3D-Beam software. The warping function depends greatly on the geometry of the cross-sectional shape. We assume the shape of the D-spar is "similar" to the shape of a rectangular section, therefore, a simple bi-linear warping function was implemented in the 3D-Beam.

The torsion-related warping, as seen in Figure 13, generally increases the α interaction parameter. The changes in the α values come from the reduction in

“GJ” and increase in the “coupling” stiffness, while the “EI” remains unchanged. For other cross-section shapes, we expect the α will change if the torsion-related warping is included.

Others

The α interaction parameter is a relative value, because it is just a square-root ratio of the coupling term to the cross product of the “EI” and “GJ”. It is possible to find two or more configurations of the ply lay-up having different cross-coupling stiffnesses, “EI” and “GJ”, but having the same α values. Figure 6 has already implicitly indicated such combinations of “coupling” stiffness, “EI” and “GJ”, that can give rise to the same α value. The control parameter for this case is the ratio of the volume of the anisotropic lay-up to the volume of the orthotropic lay-up.

For some cases, the control parameter may not be obvious. For example, the following two lay-ups, a) $[\theta_5/0_5]_S$ and b) $[\theta_4/(0/90)_3]_S$, have similar α values but different stiffness terms as shown in Figure 14. Such configurations are, in fact, found by trial-and-error.

The other observation is that “EI” and “GJ” are symmetric terms, since the terms do not change as the sign of the lay-up angle (θ) changes. However, the bend-twist coupling term will change sign if the sign of the ply angle changes. Therefore, we can make use of such features to design the lay-up configurations that have the same “EI” and “GJ” but different α values as seen in Figure 15. In this case, the key parameter for such designs is the angle ply lay-up.

SUMMARY

We identified two key parameters that significantly affect the magnitude of α in the theoretical evaluation. The two key parameters are the ply orientation angle and the materials of the laminate. A higher α value is achieved for the ply angle range between 15° and 30° . A higher α value can also be obtained by using a high-performance laminate such as Graphite/Epoxy.

We also looked into various parameters that affect the magnitude of α in the numerical evaluation. Among the parameters studied, the three key parameters are the ply orientation angle, the laminate material and the volume of anisotropy lay-up relative to the volume of orthotropic lay-up. A hybrid material lay-up will increase α if we are starting with a soft material. Other parameters such as the geometry, the inclusion of the internal rib, the mixture of the extension-twist and bend-twist lay-up, change the magnitude of the α ,

but the effect is not significant. Torsion-related warping can have a large effect on estimates of α . However, the effect depends on the shape of the cross section. In the selected D-spar, the effect from warping is marginal but tends to increase the α estimate.

We also realized through this study that the α interaction parameter is a relative value. There are many ways (configurations) to get the same α with different values of the stiffness terms.

REFERENCES

- [1] T. Weisshaar, "Aeroelastic Tailoring – Creative Uses of Unusual Materials," AIAA Paper No. 87-0976-CP, 1987.
- [2] Edward C. Smith & Inderjit Chopra, "Formulation and Evaluation of an Analytical Model for Composite Box-Beams," AIAA-90-0962-CP, 1990.
- [3] Ramesh Chandra, Alan D. Stemple, and Inderjit Chopra, "Thin-Walled Composite Beams Under Bending, Torsional, and Extensional Loads," *Journal of Aircraft*, Vol. 27, No. 7, July 1990.
- [4] H.J.T. Kooijman, "Bending-Torsion Coupling of a Wind Turbine Rotor Blade," ECN-I-96-060, December 1996.
- [5] Don W. Lobitz and Paul S. Veers, "Aeroelastic Behavior of Twist-Coupled HAWT Blades," AIAA-98-0029, January 1998.
- [6] Stephen W. Tsai and H. Thomas Hahn, *Introduction to Composite Materials*, Technomic Publishing Company, Inc., 1980.

ACKNOWLEDGEMENT

This work was initiated and supported by Sandia National Laboratories, Contract No. BB-6066; Technical Monitor Dr. Paul S. Veers.

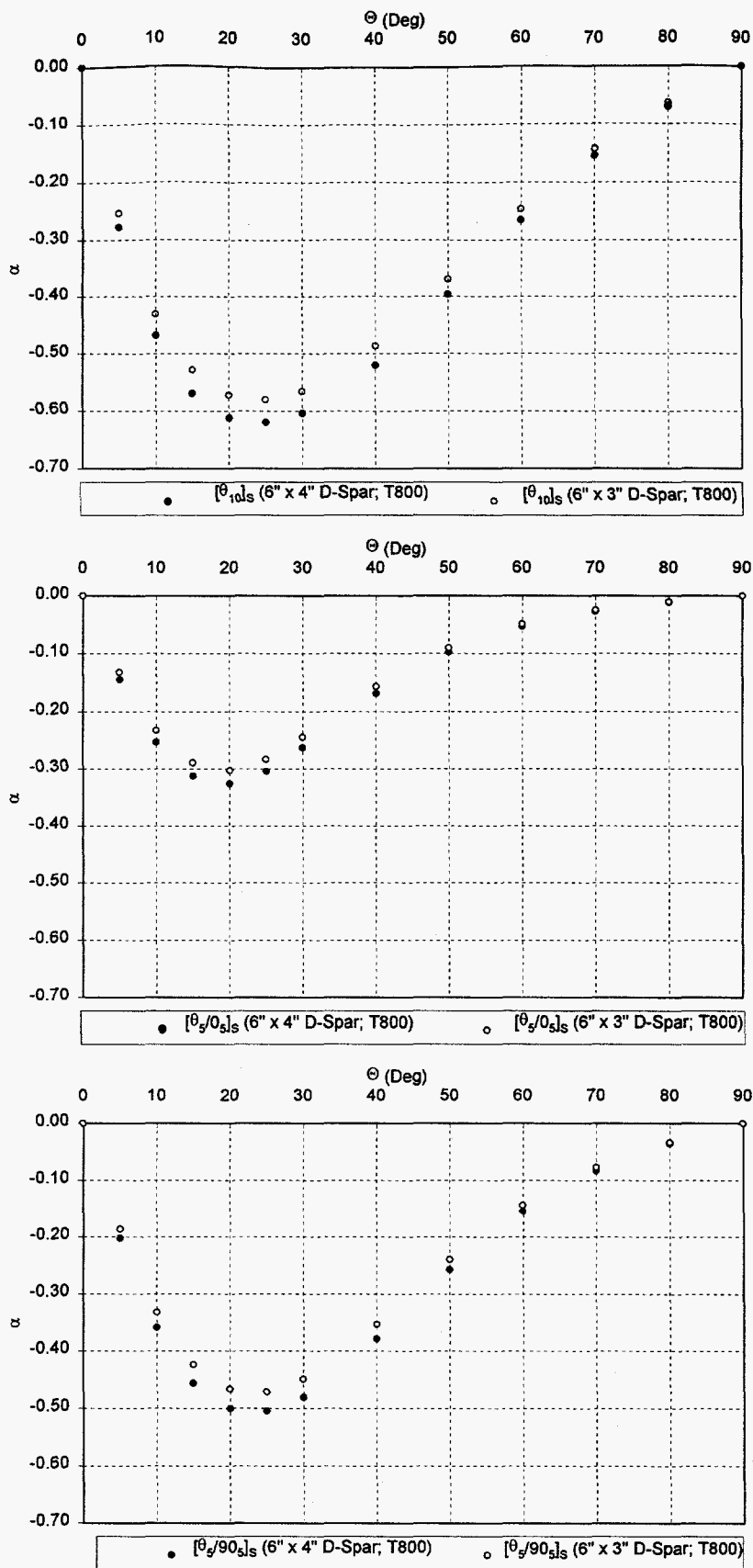


Figure 3a The Effect Of Geometry on α Interaction Parameter

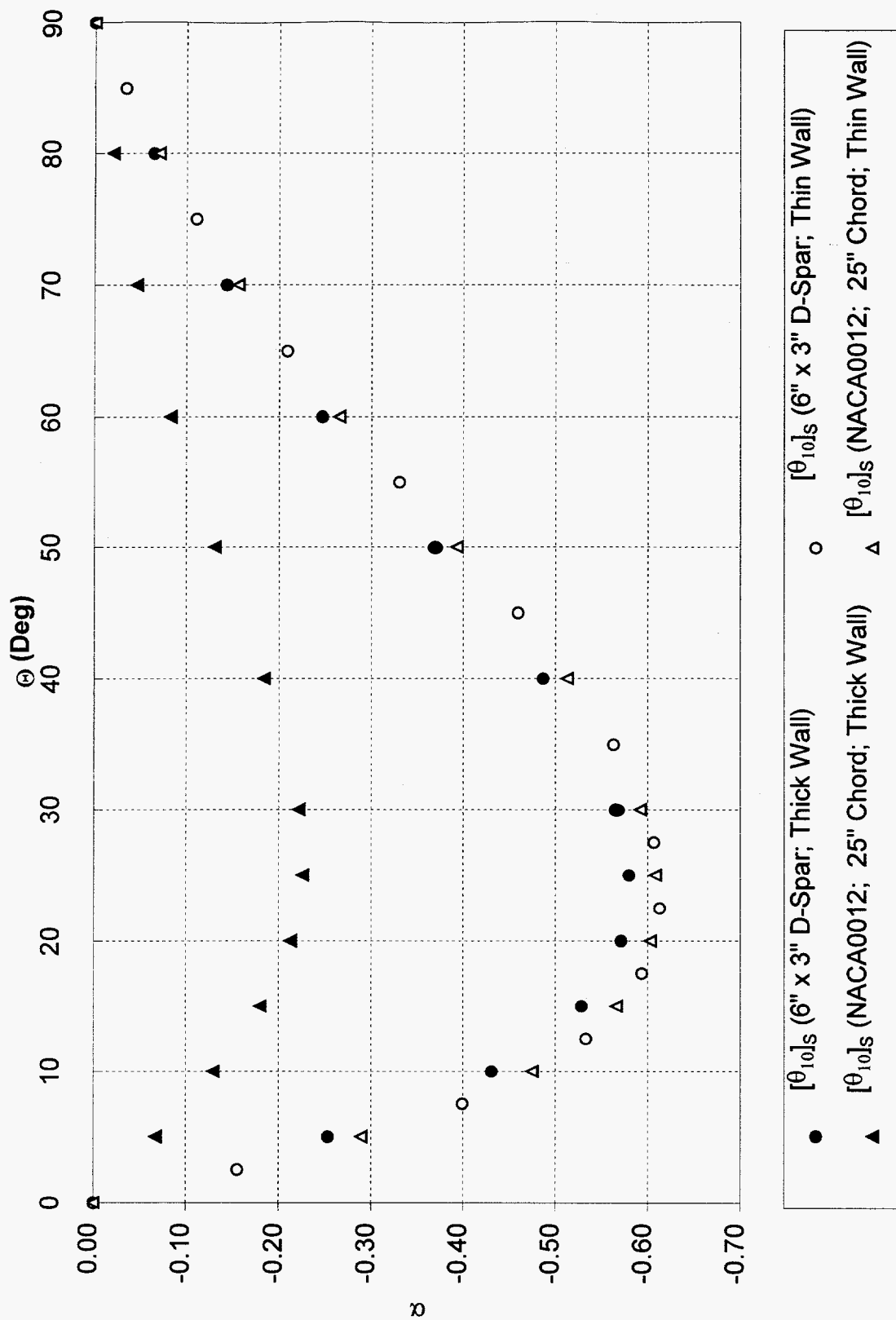


Figure 3b The Effects of Thick/Thin Wall Assumption on α Interaction Parameter

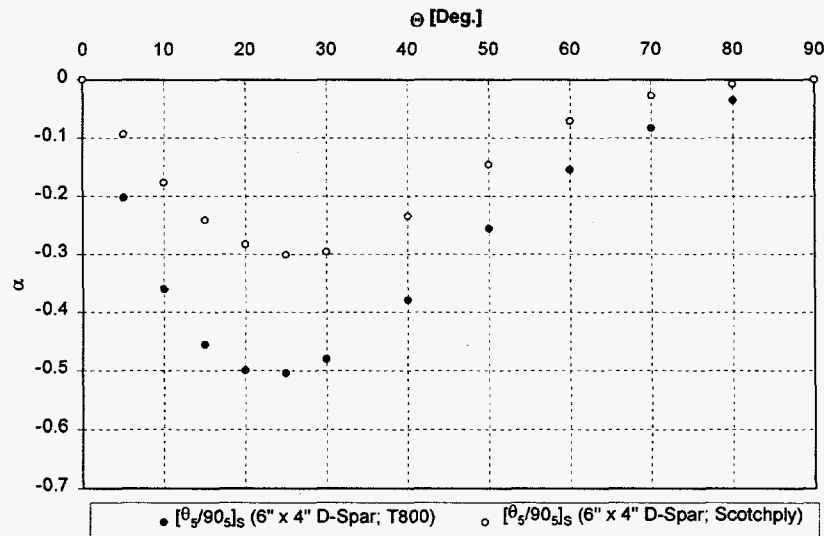
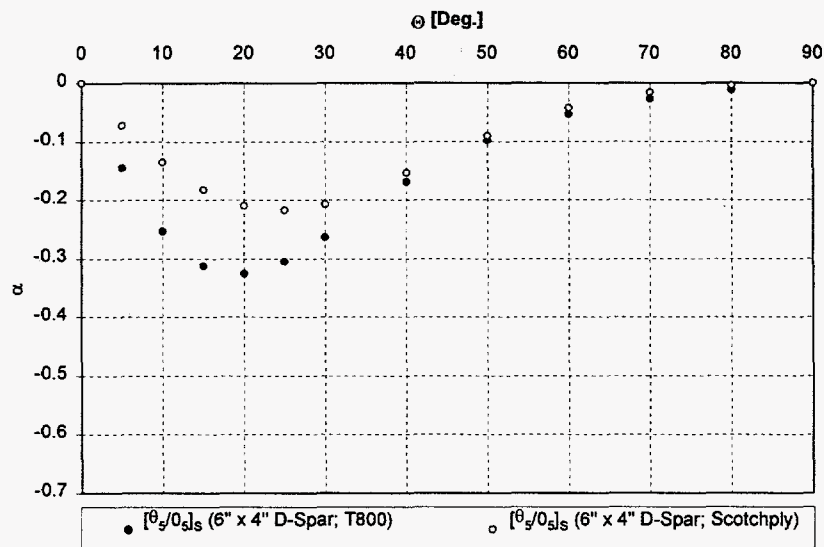
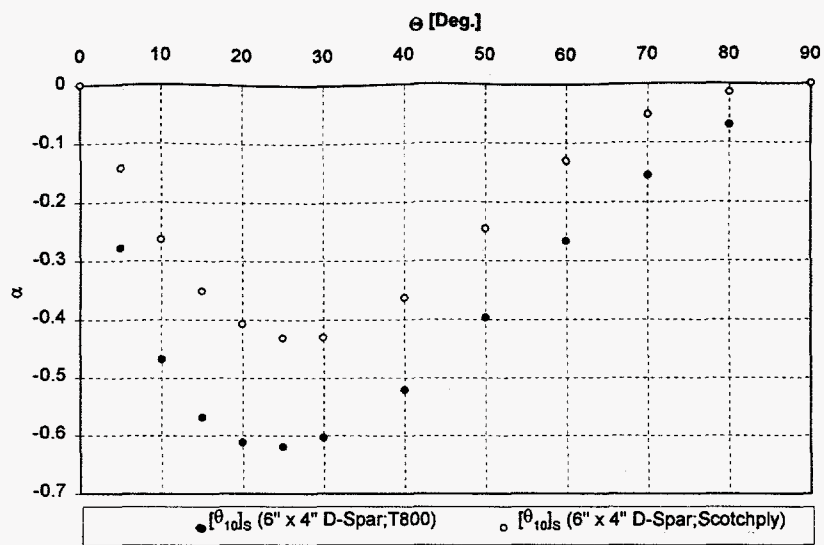


Figure 4 The Effects of Materials on α Interaction Parameter

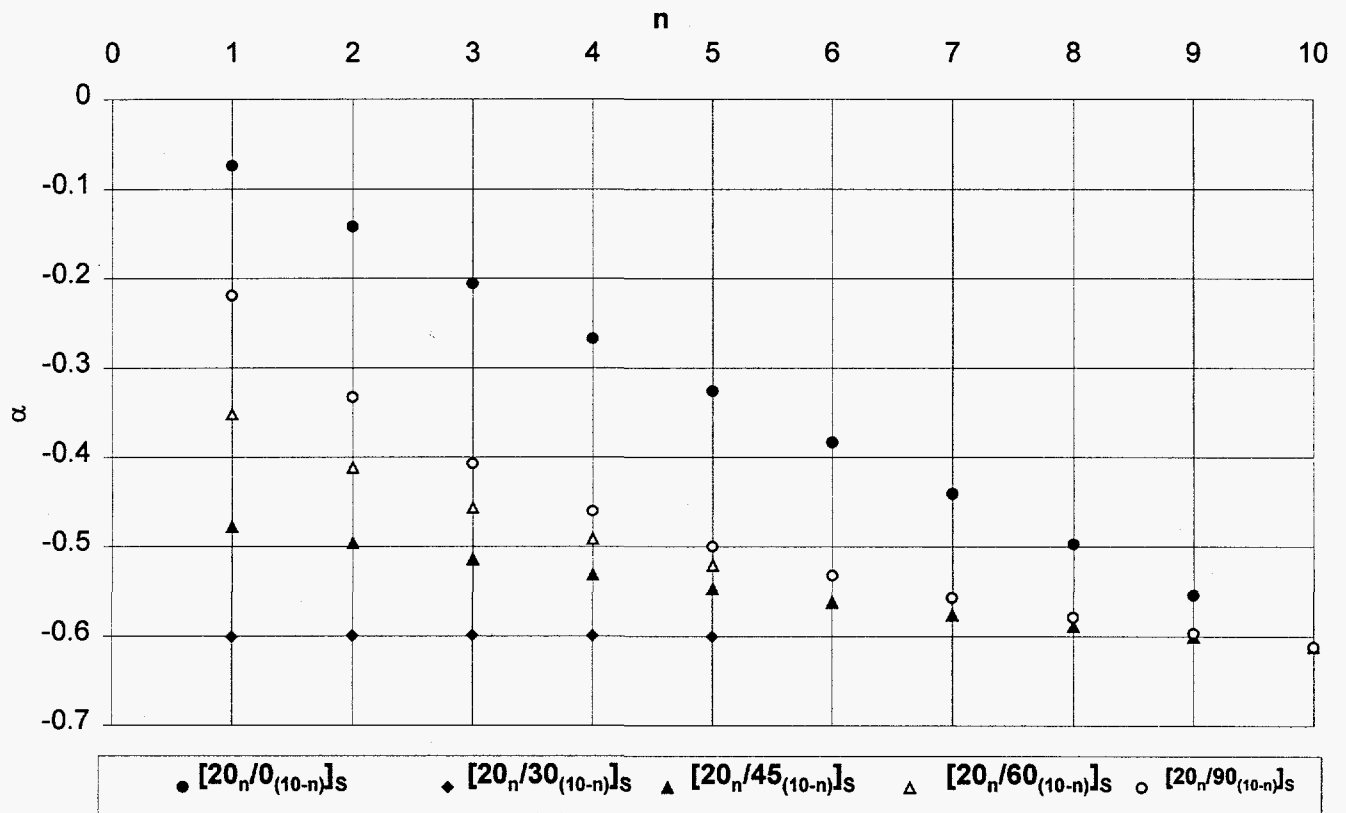
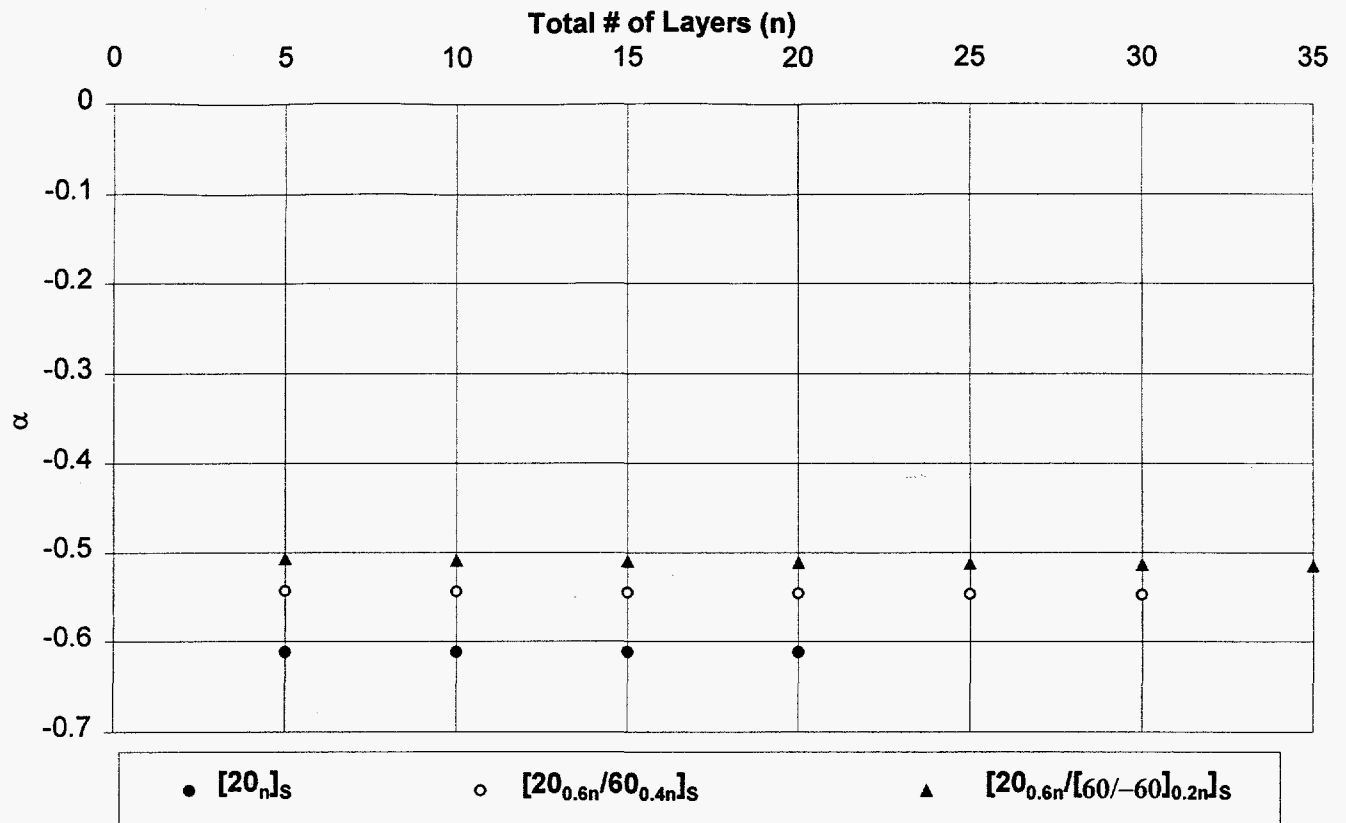


Figure 5 The Effects of Ply Thickness & Distribution for 6" x 4" D-Spar

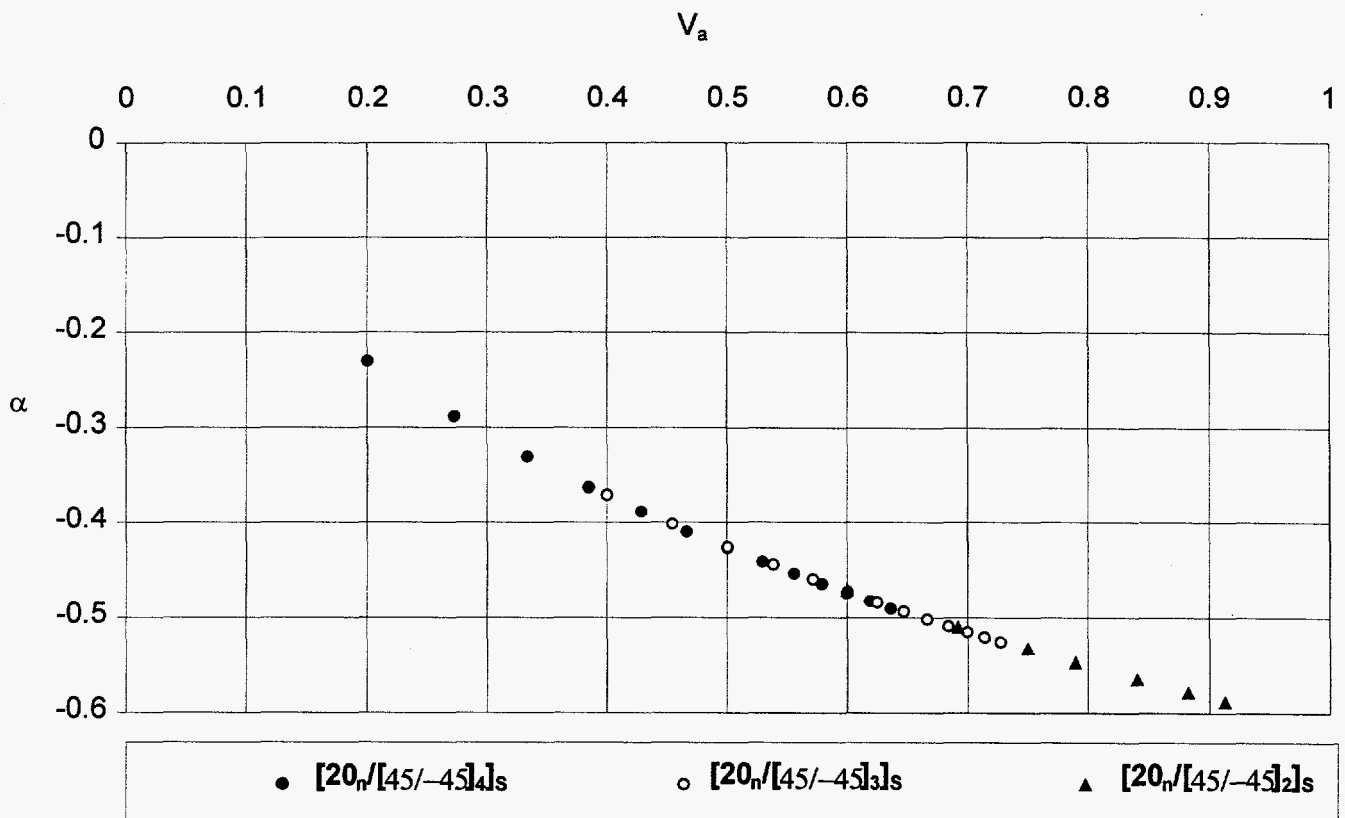
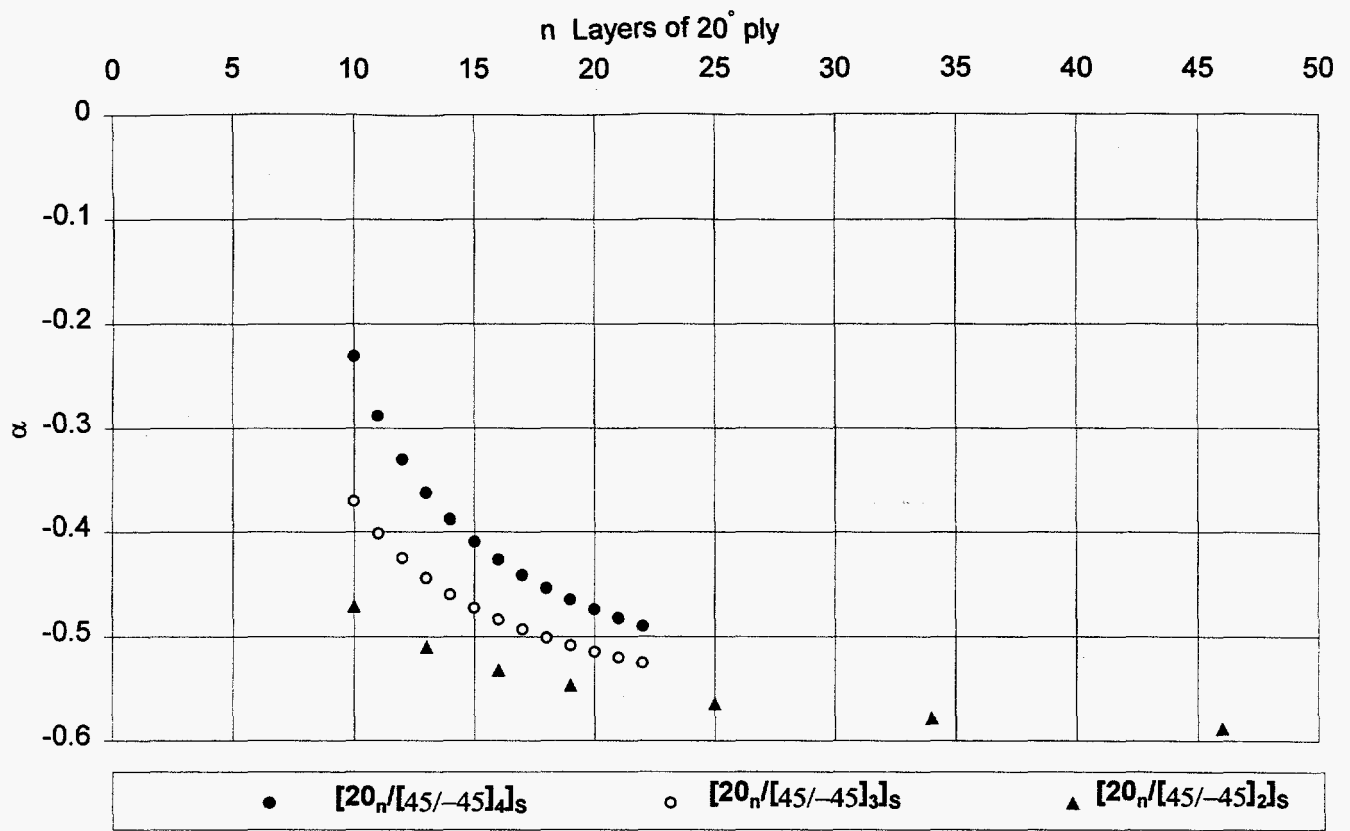


Figure 6 The Effects of Volumetry of the Anisotropy on α for 6" x 4" D-Spar

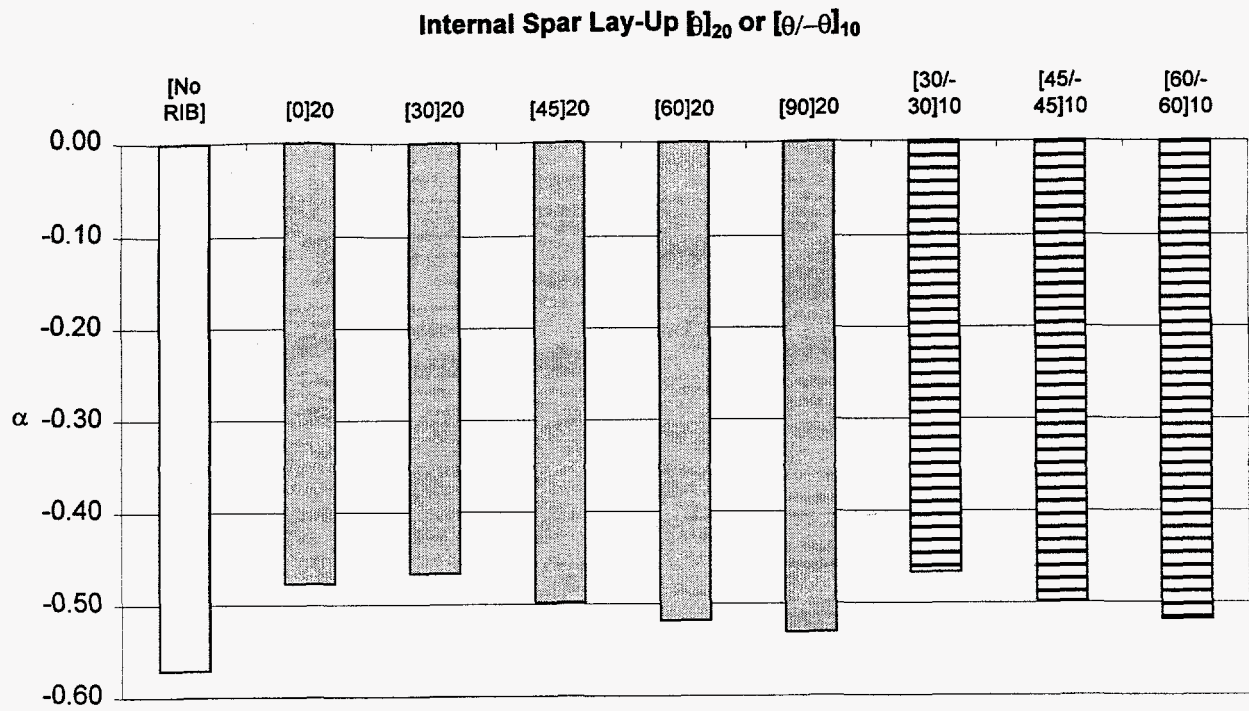


Figure 9a The Effect of Internal Spar Ply Orientation (D-spar lay-up : $[20]_{10}$)

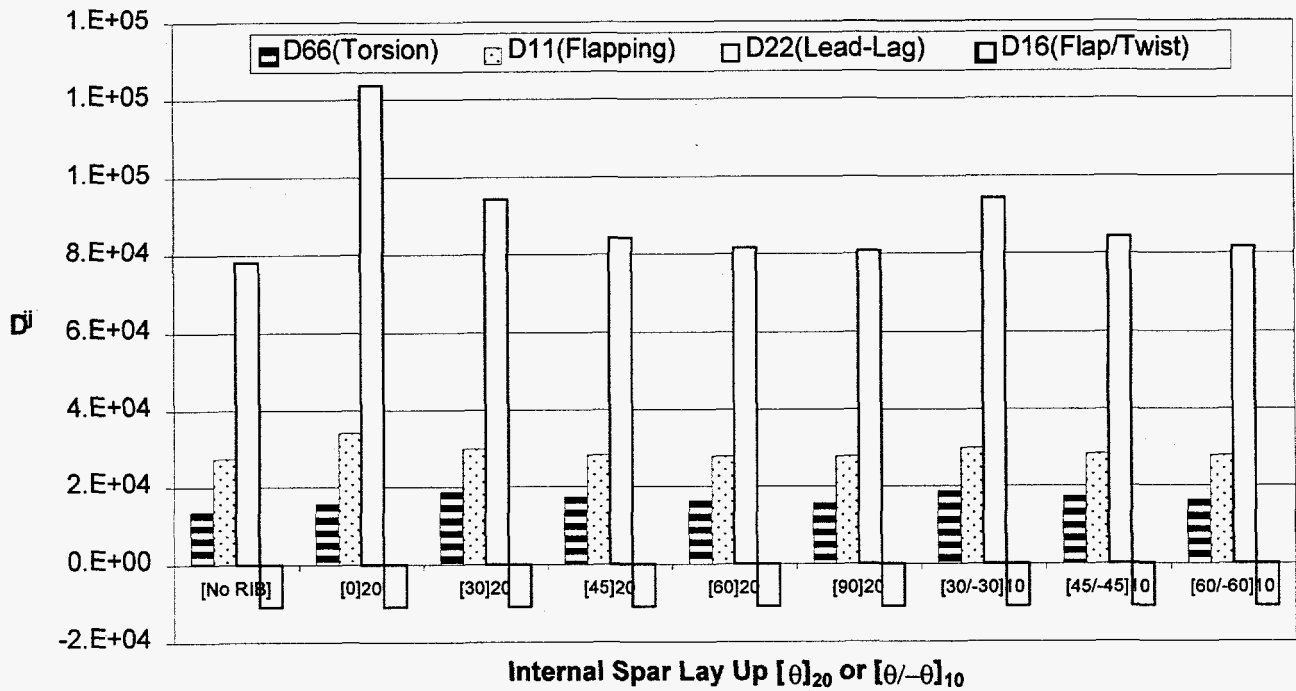


Figure 9b The Effect of Internal Spar Ply Orientation (D-spar lay-up : $[20]_{10}$)

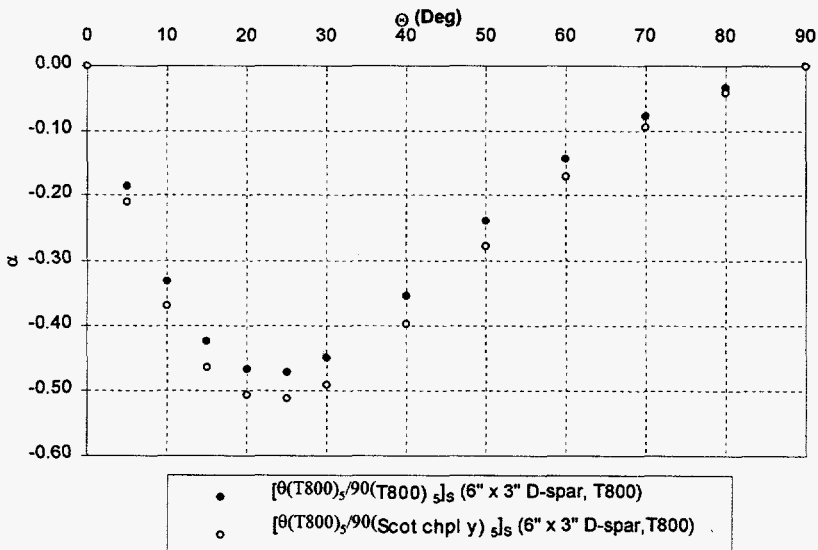
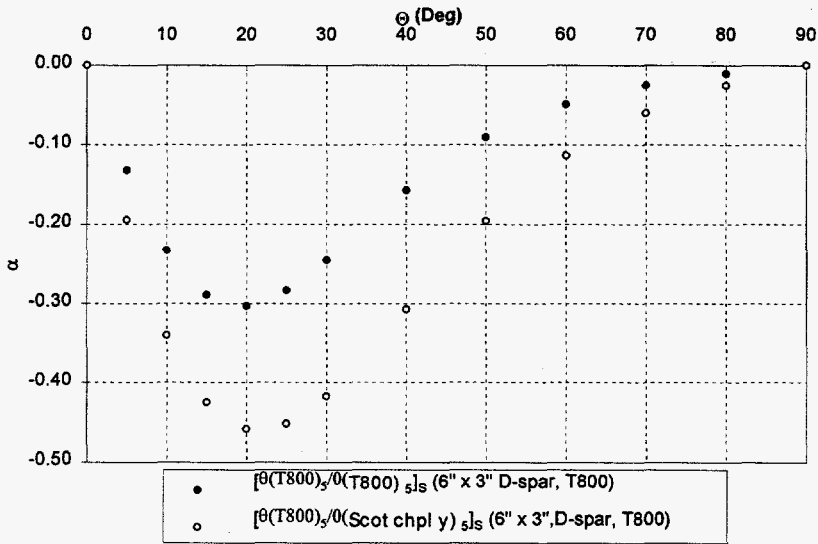
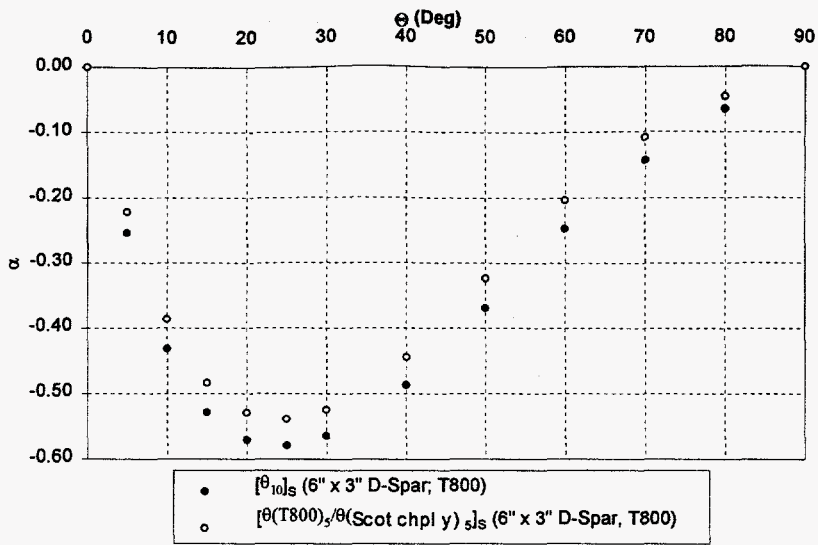
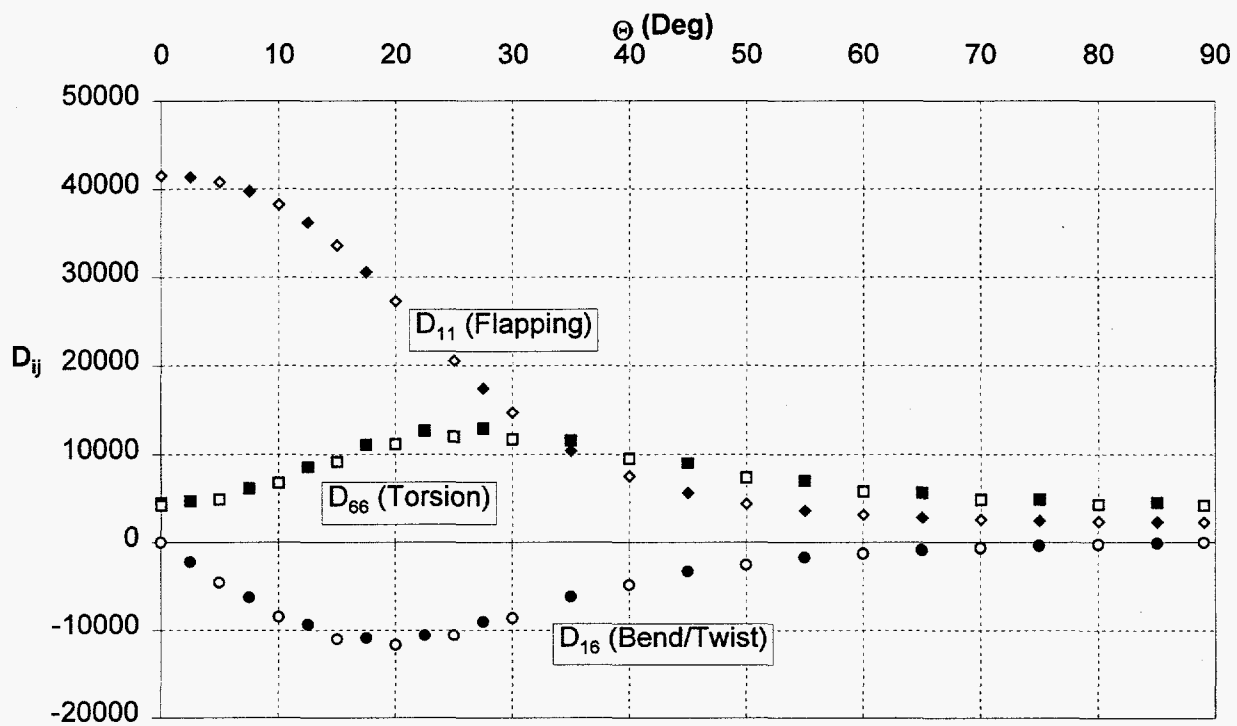
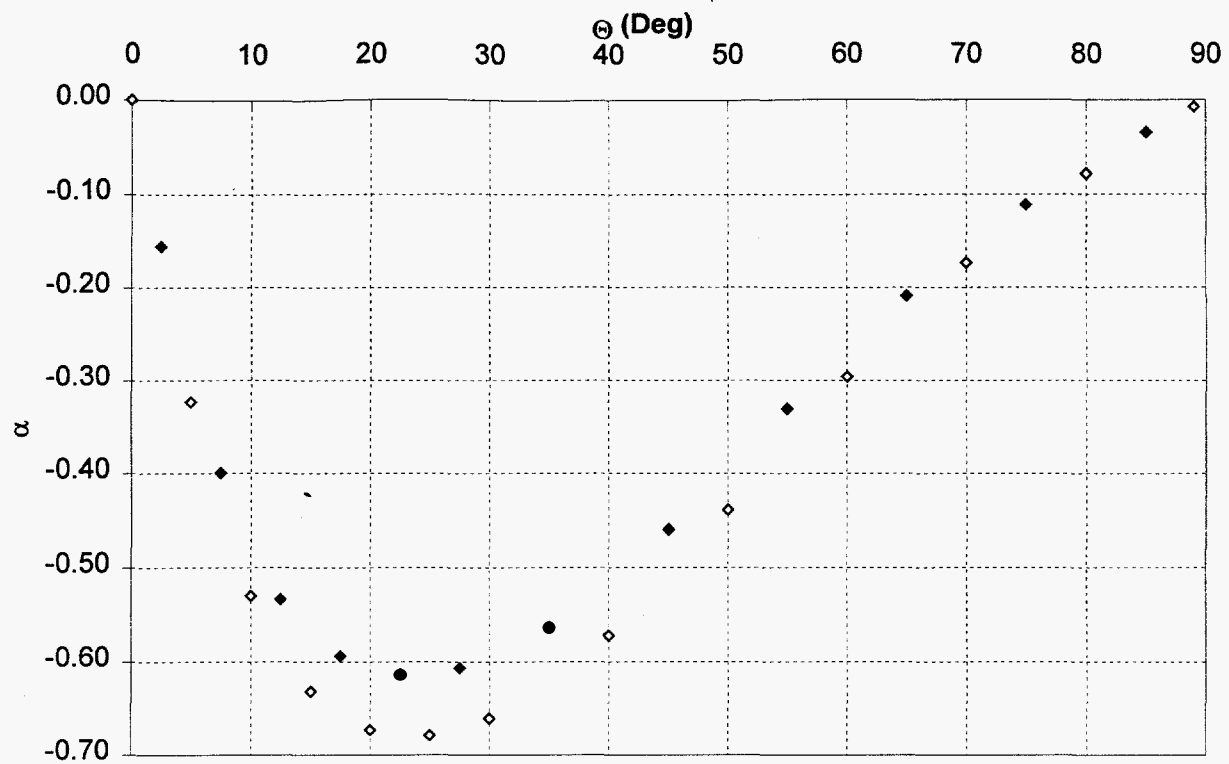


Figure 10 The Effect of Hybrid Materials on α Interaction Parameter



Solid Symbol : $[\theta_{10}]_S$ (6" x 3" D-Spar; T800)

Hollow Symbol : $[\theta_{10}]_S$ (6" x 3" D-Spar; T800; Warping)

Figure 13 The Effect of Torsion Related Warping on α and Stiffness Distribution

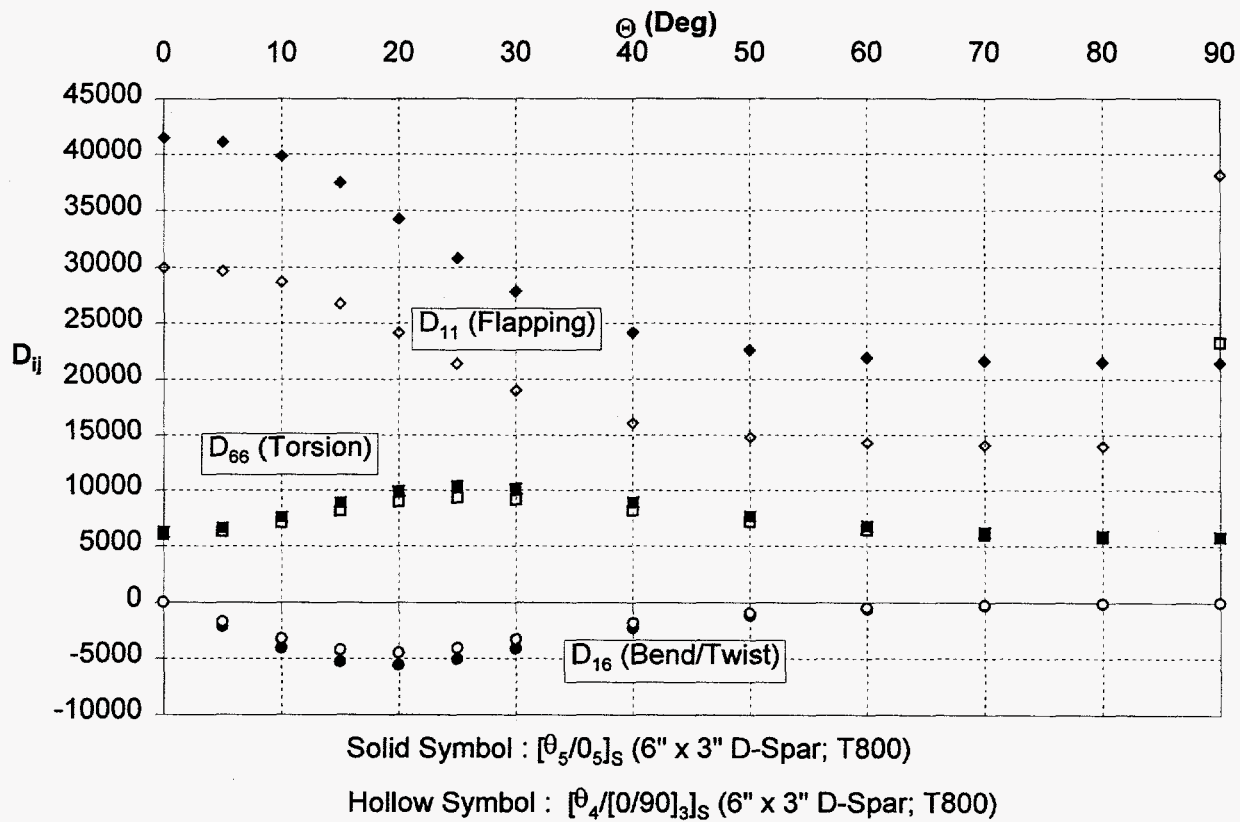
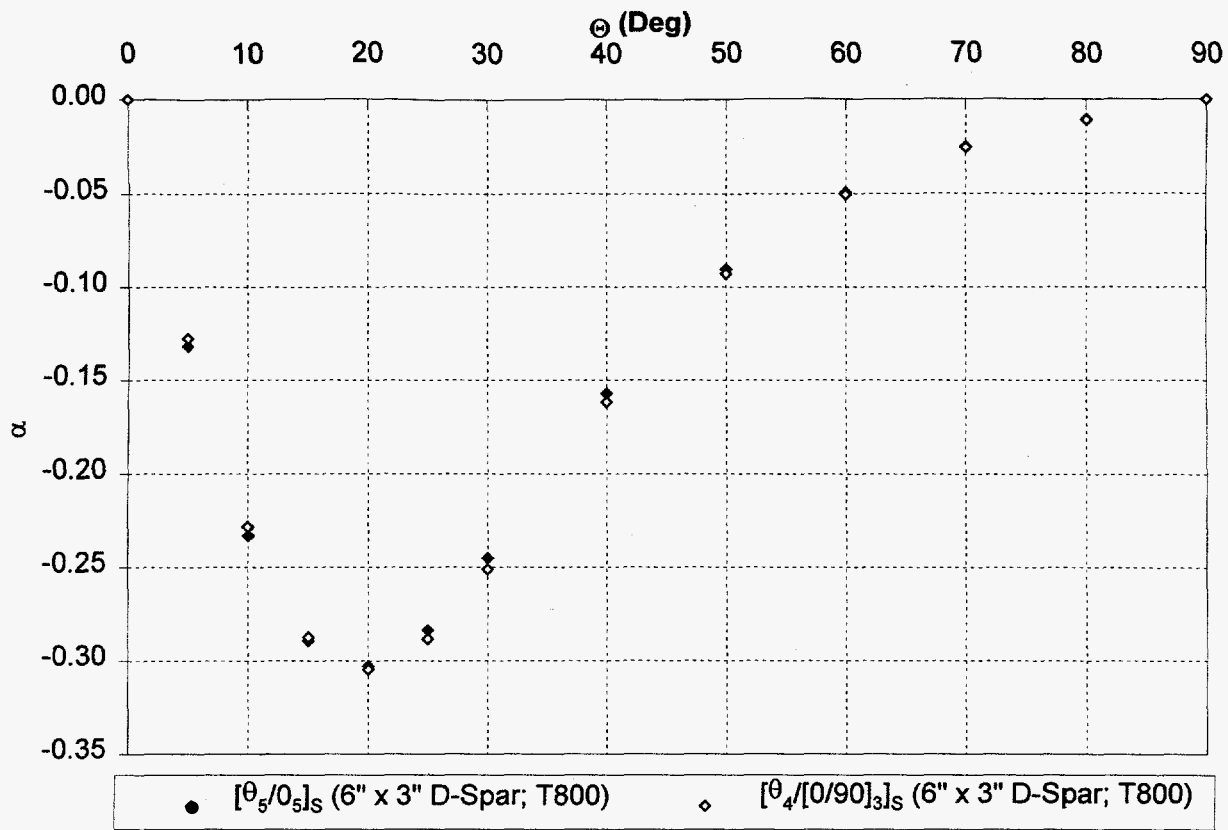


Figure 14 The Configuration that Exhibits Close α values but Different "EI" & "GJ"

D Spar {[20_(20-2n)/[20/-20]_n]_s (6" x 3")}

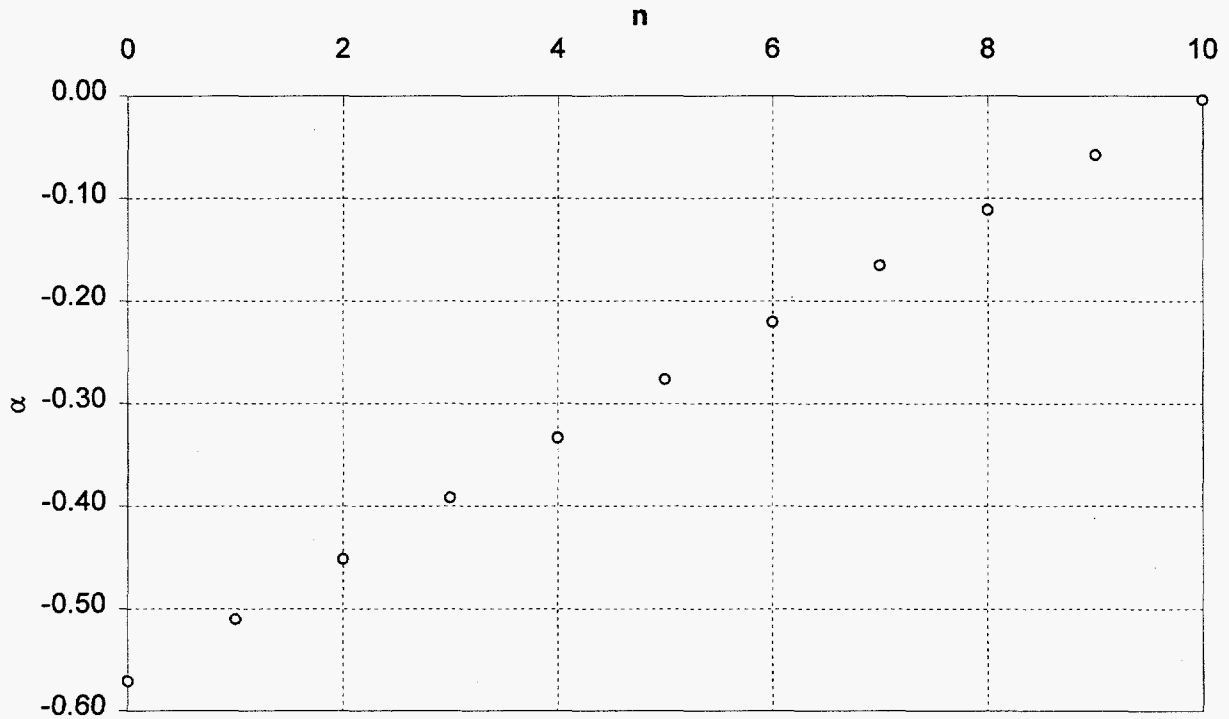
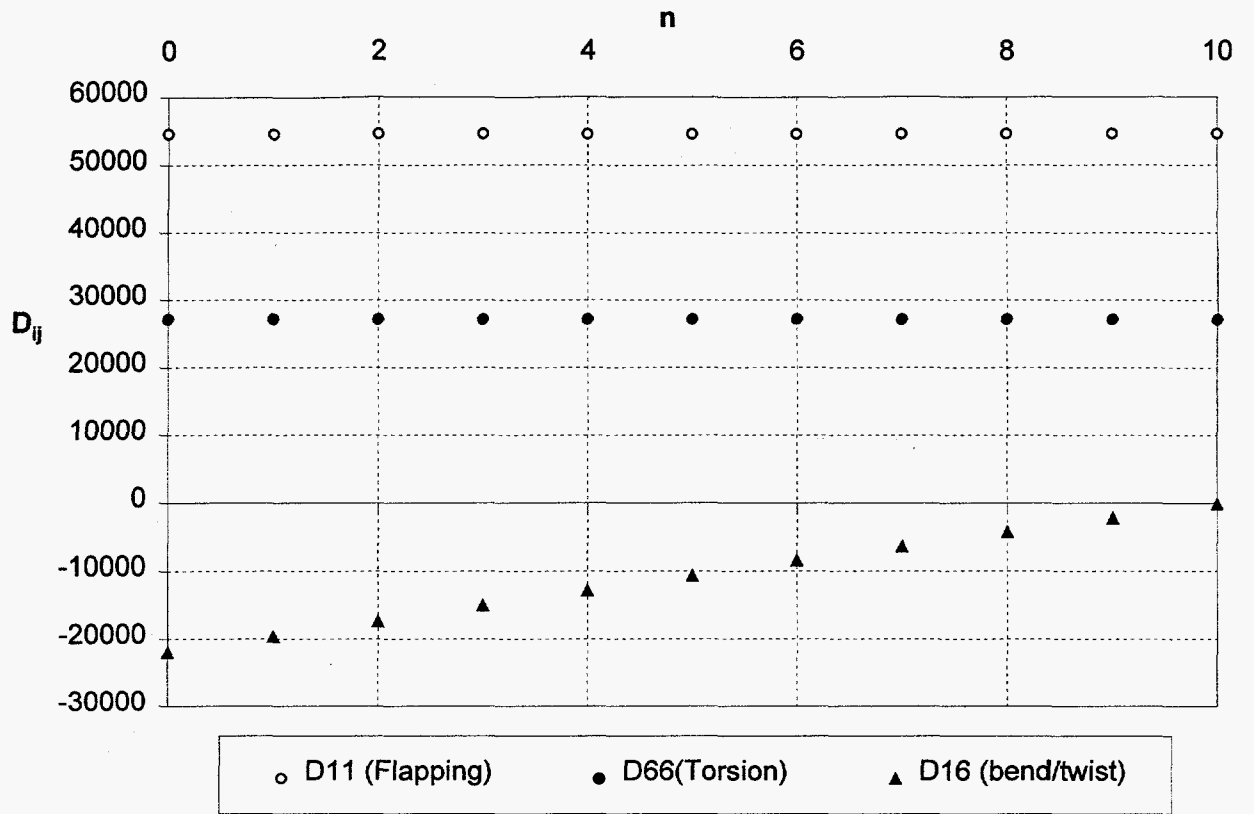


Figure 15 The Configuration that Exhibits the Same "EI" & "GJ" but Different α Values